ACS Medicinal Chemistry Letters

pubs.acs.org/acsmedchemlett Letter

Progress in the Field of Aldehyde Dehydrogenase Inhibitors: Novel Imidazo[1,2-*a*]pyridines against the 1A Family

Luca Quattrini,[‖] Edoardo Luigi Maria Gelardi,[‖] Giovanni Petrarolo, Giorgia Colombo, Davide Maria Ferraris, Francesca Picarazzi, Menico Rizzi, Silvia Garavaglia,* and Concettina La Motta*

Cite This: *ACS Med. Chem. Lett.* 2020, 11, 963–970 Read Online

ACCESS | Metrics & More | Article Recommendations | Supporting Information

ABSTRACT: Members of the aldehyde dehydrogenase 1A family are commonly acknowledged as hallmarks of cancer stem cells, and their overexpression is significantly associated with poor prognosis in different types of malignancies. Accordingly, treatments targeting these enzymes may represent a successful strategy to fight cancer. In this work we describe a novel series of imidazo[1,2-*a*]pyridines, designed as aldehyde dehydrogenase inhibitors by means of a structure-based optimization of a previously developed lead. The novel compounds were evaluated *in vitro* for their activity and selectivity against the three isoforms of the ALDH1A family and investigated through crystallization and modeling studies for their ability to interact with the catalytic site of the 1A3 isoform. Compound **3f** emerged as the first in class submicromolar competitive inhibitor of the target enzyme.

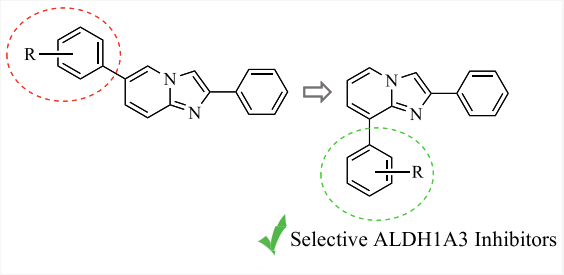

KEYWORDS: *Aldehyde dehydrogenases, aldehyde dehydrogenase inhibitors, ALDH1A1, ALDH1A2, ALDH1A3, imidazo[1,2-a]pyridines*

Aldehyde dehydrogenases (ALDHs) comprise a superfamily of 19 enzymatic NAD(P$^+$) dependent isoforms characterized by distinctive subcellular localization, chemical structure, and substrate binding. They all catalyze the irreversible oxidation of both endogenous and exogenous aldehydes to the corresponding carboxylic acids and CoA esters, thus playing a key role in a wide spectrum of biological functions.[1] The ALDH1A subfamily, including the ALDH1A1, ALDH1A2, and ALDH1A3 isoforms, turns the vitamin A metabolite retinal into all-trans retinoic acid (ATRA), 9-cis retinoic acid (9-cis-RA), and 13-cis retinoic acid (13-cis-RA), having a major role in regulating gene expression. Indeed, to date, more than 530 genes have been reported as regulatory targets of RAs, being modulated by these ligands either directly, thanks to the RA response element (RARE) sequence in their promoter, or indirectly, through transcriptional intermediaries.[2] Such a massive modulation gives the sense of RA as a crucial mediator and, above all, testifies the functional role of the ALDH1A family in regulating cell morphogenesis and development. Actually, these enzymes are highly expressed in embryonal tissues and in cells showing a stem-like phenotype, including both normal stem cells and cancer stem cells (CSCs).[3]

Besides acting as a marker for the identification of colonic stem cells, members of the ALDH1A family are able to affect stem cell vitality regulating self-renewal, differentiation, and expansion. In the case of CSCs, ALDH activity is decisive for tumor progression and invasion, so much that a high expression of the different ALDH1A isoforms often has a prognostic value for poor clinical outcomes.[4,5] ALDH1A1 activation has been observed in the stem-like population of multiple myeloma and acute myeloid leukemia.[6] Moreover, high levels of this isoenzyme predict negative prognosis in patients with esophageal squamous cell carcinoma[7] and prostate cancer[8] and are reported as responsible for platinum resistance of ovarian cancer cells.[9] ALDH1A3 overexpression is associated with worse prognosis in aggressive and/or triple-negative breast cancer,[10,11] and it is also responsible for tumorigenicity in nonsmall cell lung cancer.[12] In addition, increased expression of this isoform endorses high grade gliomas.[13]

Accordingly, targeting these enzymes with suitably designed inhibitors represents a successful strategy to fight CSCs, resulting in an innovative and groundbreaking molecular treatment of cancer.[14]

We recently developed a novel series of ALDH inhibitors bearing the 2,6-diphenyl-imidazo[1,2-*a*]pyridine core structure, developed as prototypical drug candidates to fight glioma stem-like cells (GSCs). Pursuing a rational optimization of the representative hit GA11[15] (Chart 1) and making use of distinctive substitution patterns on the two pendant phenyl

Special Issue: In Memory of Maurizio Botta: His Vision of Medicinal Chemistry

Received: January 3, 2020
Accepted: March 25, 2020
Published: March 25, 2020

https://dx.doi.org/10.1021/acsmedchemlett.9b00686
ACS Med. Chem. Lett. 2020, 11, 963–970

Chart 1

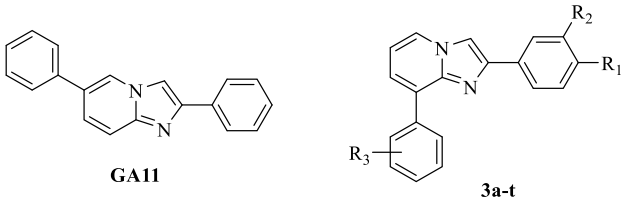

rings, we succeeded in modulating the functional profile of the synthesized compounds obtaining fully selective derivatives able to target either ALDH1A1 isoenzyme or the parent ALDH1A3.[16] Besides an unquestionable significance as pharmacological tools, the novel compounds displayed also a relevant functional efficacy. Indeed, when tested against well-characterized patient-derived GSCs, representative examples of ALDH1A3 inhibitors displayed antiproliferative efficacy in the nanomolar/picomolar range, thus imposing themselves as novel prototypes of drug candidates deserving further investigation.

A close inspection of the complex obtained cocrystallizing GA11 with the human recombinant ALDH1A3 revealed that the reference compound gets settled at the entrance of the catalytic tunnel of the enzyme.[16] Arranged in this pose, GA11 forecloses access to the natural substrate retinal, thus allowing inhibition of the catalytic activity of the enzyme but was proved to occupy only partly the enzyme site, thus offering interesting clues for the rational optimization of this class of compounds. In particular, the obtained binding mode lead to speculation that shifting the 6-phenyl ring to the 8-position could come in very handy to cast these derivatives into the deepest part of the enzyme binding site, in close proximity to the key catalytic residue C314. Prompted by this speculation, we embarked in the synthesis of a novel series of 8-substituted derivatives, **3a−t** (Chart 1), which were investigated for their functional efficacy and mode of interaction against the human recombinant isoforms of the ALDH1A family.

RESULTS AND DISCUSSION

Chemistry. The synthesis of the target inhibitors **3a−t** was performed as depicted in Scheme 1. Reaction of the commercially available 2-amino-3-bromo pyridine **1** with the suitably substituted 2-bromo-1-phenylethan-1-one, in the presence of potassium carbonate, gave the corresponding key intermediates 8-bromo-2-phenylimidazo[1,2-*a*]pyridines **2a−d**, which provided the desired inhibitors **3a−t** by coupling reactions with differently substituted phenylboronic acids, performed in the presence of $Pd(OAc)_2$ and PPh_3 as the catalysts.

Functional Evaluation of the Novel Imidazo[1,2-*a*]pyridine Derivatives. All the synthesized compounds, characterized by different substitution patterns on both the 2- and 8-phenyl rings, were tested *in vitro* for their efficacy against the human recombinant ALDH1A3 and selectivity toward the parent isoforms ALDH1A1 and ALDH1A2. They were preliminarily screened at a single concentration of 25 μM (Figure 1). Compounds showing the best inhibitory efficacy were further investigated for their kinetic parameters, including IC_{50} and K_i values. Results obtained allowed us to sketch some structure−activity relationships. In particular, moving from the unsubstituted **3a** (IC_{50} 80.6 ± 1.8 μM, Table 1), the most significant increase in the inhibitory efficacy of the novel series was obtained through the insertion of electron-withdrawing substituents in the *para* position of the 8-phenyl ring. Actually, both compound **3b** (IC_{50} 6.0 ± 1.3 μM, Table 1), carrying a fluoro atom, and compound **3c** (IC_{50} 5.5 ± 1.4 μM, Table 1), carrying a chloro atom, turned out to be almost ten times more potent than the lead **3a**. An even better inhibitory profile was obtained through the insertion of a methoxycarbonyl fragment as in derivative **3f** (IC_{50} 0.66 ± 1.3 μM, Table 1), whose activity in the submicromolar range increased a hundredfold compared to the unsubstituted **3a**. Interesting functional results were also obtained when additional substituents, like methyl and methoxyl groups, were added on the 2-phenyl ring. Among the investigated combinations, the one including a methoxy

Scheme 1. Synthesis of 8-Substituted-Imidazo[1,2-a]pyridine Derivatives 3a−t[a]

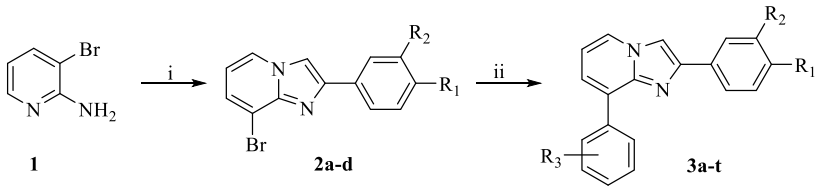

a: R_1=H, R_2=H
b: R_1=CH_3, R_2=H
c: R_1=OCH_3, R_2=H
d: R_1=H, R_2=OCH_3

a: R_1=H, R_2=H, R_3=H
b: R_1=H, R_2=H, R_3=4-F
c: R_1=H, R_2=H, R_3=4-Cl
d: R_1=H, R_2=H, R_3=4-$CH_2CH(CH_3)_2$
e: R_1=H, R_2=H, R_3=4-$OCH_2COC_6H_5$
f: R_1=H, R_2=H, R_3=4-$COOCH_3$
g: R_1=H, R_2=H, R_3=4-C_6H_5
h: R_1=CH_3, R_2=H, R_3=H
i: R_1=CH_3, R_2=H, R_3=4-F
j: R_1=CH_3, R_2=H, R_3=4-Cl
k: R_1=OCH_3, R_2=H, R_3=4-F
l: R_1=OCH_3, R_2=H, R_3=4-Cl
m: R_1=OCH_3, R_2=H, R_3=3,5-diOCH_3
n: R_1=OCH_3, R_2=H, R_3=3,4,5-triOCH_3
o: R_1=OCH_3, R_2=H, R_3=4-$COOCH_3$
p: R_1=OCH_3, R_2=H, R_3=4-C_6H_5
q: R_1=H, R_2=OCH_3, R_3=4-F
r: R_1=H, R_2=OCH_3, R_3=4-Cl
s: R_1=H, R_2=OCH_3, R_3=3,4,5-triOCH_3
t: R_1=H, R_2=OCH_3, R_3=4-C_6H_5

[a]Reagents and conditions: (i) 2-Bromo-1-(4-(3)substituted phenyl)ethan-1-one, K_2CO_3, Δ; (ii) Substitued-phenylboronic acid, $Pd(OAc)_2$, PPh_3, K_2CO_3, Δ.

https://dx.doi.org/10.1021/acsmedchemlett.9b00686
ACS Med. Chem. Lett. 2020, 11, 963−970

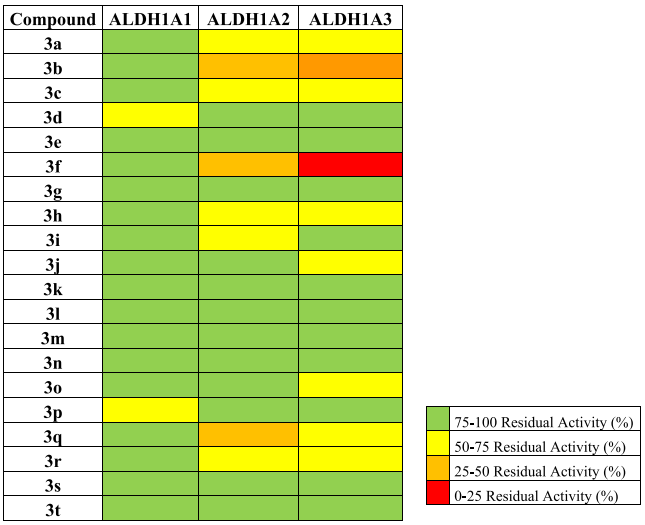

Figure 1. Heat map of ALDH1As residual activities in the presence of 8-substituted-imidazo[1,2-*a*]pyridine derivatives **3a**−**t**.

fragment in the *meta* position of the 2-phenyl ring, as in compounds **3q** (IC_{50} 7.2 ± 1.5 μM, Table 1) and **3r** (IC_{50} 4.3 ± 1.6 μM, Table 1), turned out to be the most effective one, helping to keep the inhibitory activity in the low micromolar range.

An in depth biochemical investigation carried out on the most effective derivatives, **3c** and **3f**, revealed the fully competitive inhibitory profile of the novel compounds. They both were highly selective against the human isoenzyme ALDH1A3 (**3c**, K*i* 8.7 ± 0.9 μM, **3f**, K*i* 0.12 ± 0.01 μM) with respect to the parent 1A1 (**3c**, K*i* 168.3 ± 2.6 μM, **3f**, K*i* 79.5 ± 1.8 μM), but not completely toward the 1A2 isoform (**3c**, K*i* 27.6 ± 1.2 μM, **3f**, K*i* 0.92 ± 1.5 μM).

Crystallization and Molecular Modeling Studies. Compounds **3c** and **3f**, showing the best inhibitory profile of the whole series, were then investigated further, to clarify their mode of interaction with the ALDH1A3 isoform. The three-dimensional structure of human ALDH1A3 in complex with **3c** has been obtained and solved by molecular replacement, using the human ALDH1A3 atomic coordinates as a search model (PDB code: 5FHZ[17]), and refined at a resolution of 2.9 Å. The final human ALDH1A3 model contains two identical chains per asymmetric unit, arranged as a dimer, and a total of 11 solvent molecules (Table 1-SI, Supporting Information). The structure analysis confirms that the obtained **3c**−ALDH1A3 complex folds into 13 α-helices, 19 β-strands, and the connecting loops, arranged into three functional domains. Both the NAD^+ binding domain and the catalytic domain are built on a topologically related $\beta\alpha\beta$ type polypeptide fold (Figure 2A). Our crystallographic data revealed that, in all monomers, **3c** enters the catalytic tunnel projecting toward the catalytic cysteine 314 (C314). In particular, the chloride atom (Cl01) on the 8-phenyl ring contacts directly C314 through an H-bond interaction (3.26 Å) (Figure 2B). By adopting this pose, **3c** casts the 8-phenyl ring toward the side chain of the aromatic F308, I321, and N469, thus allowing $\pi-\pi$ stacking interactions which make the binding more effective. In addition, T315 stabilizes **3c** bonding through van der Waals contact. Notably, the four mentioned residues are specific of ALDH1A3 isoform and are not conserved in the other two isoenzymes (Figure 3). As they significantly contribute to define the binding pocket hosting **3c**, they give reason to the inhibitory selectivity displayed by the compound against the three isoenzymes. Moreover, the phenyl ring in position 2 of the nucleus establishes additional contacts with the protein backbone, including $\pi-\pi$ stacking interaction and van der Waals contacts with W189, T140, and R139 (Figure 2B). The mentioned residues are conserved in each of the 1A1, 1A2, and 1A3 isozymes, with this enzymatic area being the one stabilizing retinoic acid binding in the whole members of the 1A subfamily, as previously demonstrated.[17]

Different attempts to cocrystallize **3f** in complex with human recombinant ALDH1A3 were fruitless. Therefore, in the absence of a reliable crystal structure, the binding mode of **3f** within the catalytic site of ALDH1A3 has been assumed by molecular docking simulations, carried out using the GOLD program.[18] To assess the reliability of the docking protocol, the cocrystallized ligand **3c** was self-docked into the catalytic site of ALDH1A3, providing a very good agreement with the crystallographic pose (RMSD < 0.5 Å). Molecular docking simulations identified two possible, although alternative, binding modes for **3f**. The replacement of the chlorine atom with the ester moiety significantly modified the binding mode of the imidazopyridine scaffold. In the first pose (Figure 4A), the

Table 1. ALDH1As Inhibitory Activity of 8-Substituted-imidazo[1,2-*a*]pyridine Derivatives 3a−c,f,q,r

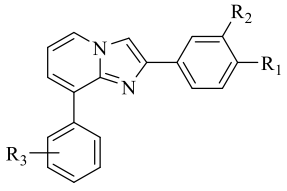

				IC_{50} (μM)[a]		
N	R_1	R_2	R_3	ALDH1A1	ALDH1A2	ALDH1A3
3a	H	H	H	n.a.[b]	61.4 ± 1.6	80.6 ± 1.8
3b	H	H	4-F	n.a.	n.a.	6.0 ± 1.3
3c	H	H	4-Cl	168.3 ± 2.6	27.6 ± 1.2	5.5 ± 1.4
3f	H	H	4-$COOCH_3$	n.a.	n.a.	0.66 ± 1.3
3q	H	OCH_3	4-F	n.a.	n.a.	7.2 ± 1.5
3r	H	OCH_3	4-Cl	n.a.	n.a.	4.3 ± 1.6

[a]IC_{50} values represent the concentration required to produce 50% enzyme inhibition. [b]Not active. No significant enzyme inhibition was observed at 25 μM.

https://dx.doi.org/10.1021/acsmedchemlett.9b00686
ACS Med. Chem. Lett. 2020, 11, 963−970

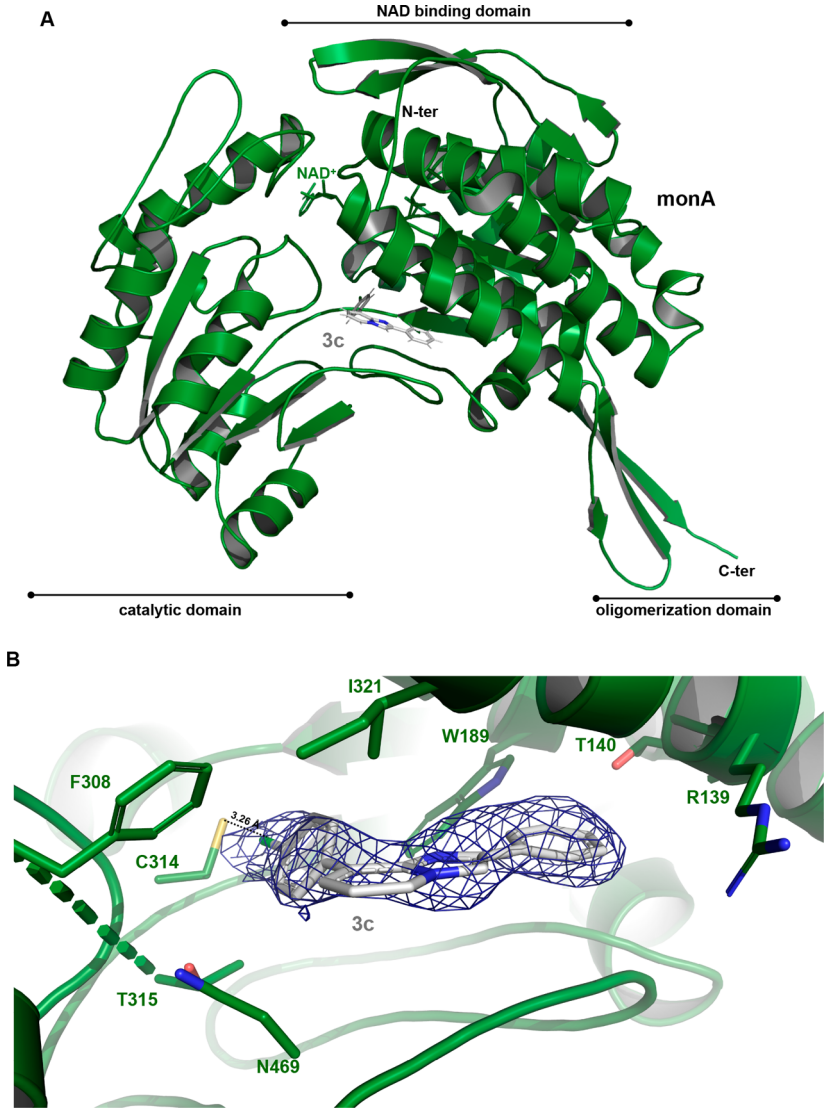

Figure 2. (A) ribbon representation of the overall structure of the monomer B ALDH1A3 (PDB code: 6TRY) with **3c** and NAD^+. Each monomer consists of three domains: the NAD binding-domain, the catalytic-domain and the oligomerization domain, all highlighted with rows. The ligands NAD^+ and **3c** are shown as green and gray sticks, respectively. (B) electron density map (2mFo-dFc) in blue, countered at 1.0 sigma, used to determine the presence of **3c** into the enzyme binding site.

phenyl ring in position 2 is oriented toward the catalytic C314 and establishes a sandwich-like and a parallel-displaced $\pi-\pi$ stacking interaction with F182 and with W189, respectively. The imidazopyridine core is accommodated into the hydrophobic pocket flanked by I132, F308, and L478, at the entrance of the catalytic tunnel, while the ester group establishes a H-bond with N469. In the second pose (Figure 4B), interactions of the phenyl group at position 2 and the imidazopyridine group remain unchanged, while the ester moiety is H-bonded to R139. It is worth mentioning that, regardless of the binding poses proposed by the GOLD program, **3f** is able to establish an additional H-bond interaction with key ALDH1A3 residues that are not present in the crystallographic binding mode of **3c**, and this gives reason for the stronger ALDH1A3 inhibitory activity of **3f**.

The obtained docking poses were further investigated by molecular dynamics (MD) simulations using Amber18.[19] Each **3f**–ALDH1A3 complex was simulated for 300 ns of unrestrained MD, while the most representative conformations were extracted from MD trajectories by cluster analysis. The docking pose shown in Figure 4A is highly destabilized in MD and converges to a new binding mode (MD simulation video, Supporting Information) in which the ester group is oriented toward the catalytic C314, while the unsubstituted phenyl ring establishes a cation$-\pi$ interaction with R139 (Figure 4C). Notably, this pose remains stable along the MD trajectory (Figure 1-SI, Supporting Information) and is highly comparable to the crystallographic pose of **3c** (Figure 2-SI, Supporting Information). The pose shown in Figure 4B, in which the ester group is H-bonded to R139, keeps the same orientation for the whole MD simulation. In the MD trajectory, **3f** loses the interaction with R139 and establishes a water-bridged H-bond with A473 (Figure 4D). The theoretical affinity of **3f** to ALDH1A3 was computed by the molecular mechanics/generalized Born surface area (MMGBSA) approach.[20] Notably, the two poses are almost isoenergetic (delta energies of binding are -33.07 ± 0.26 kcal/mol and -35.88 ± 0.47 kcal/mol for the pose shown in Figure 4C and 4D, respectively).

Overall, both crystallographic and molecular modeling studies, carried out on the representative compounds **3c** and **3f**, evidence that the novel 2,8-diphenylimidazopyridines are

https://dx.doi.org/10.1021/acsmedchemlett.9b00686
ACS Med. Chem. Lett. 2020, 11, 963−970

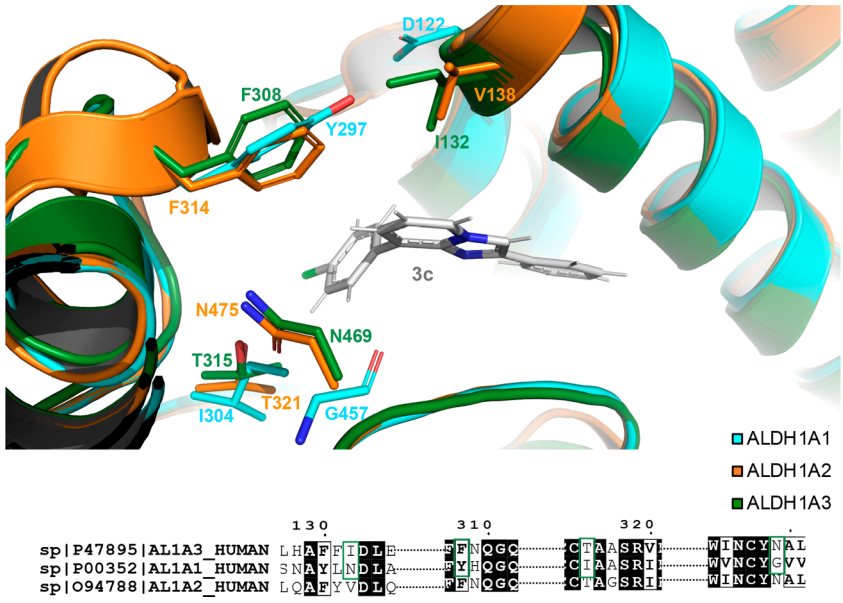

Figure 3. Superposition of inhibitor binding site between ALDH1A3 in forest green, ALDH1A1 (PDB_code: 4WB9[24]) in cyan and ALDH1A2 (PDB_code: 6ALJ[25]) in orange. The three structures maintain the same structure arrangement. Side chains of key residues, involved in the **3c**–ALDH1A3 binding (I132, F308, T315, and N469), are shown in forest green sticks. The correspondent not conserved residues of ALDH1A2 and of ALDH1A1 are represented in orange sticks and cyan sticks, respectively.

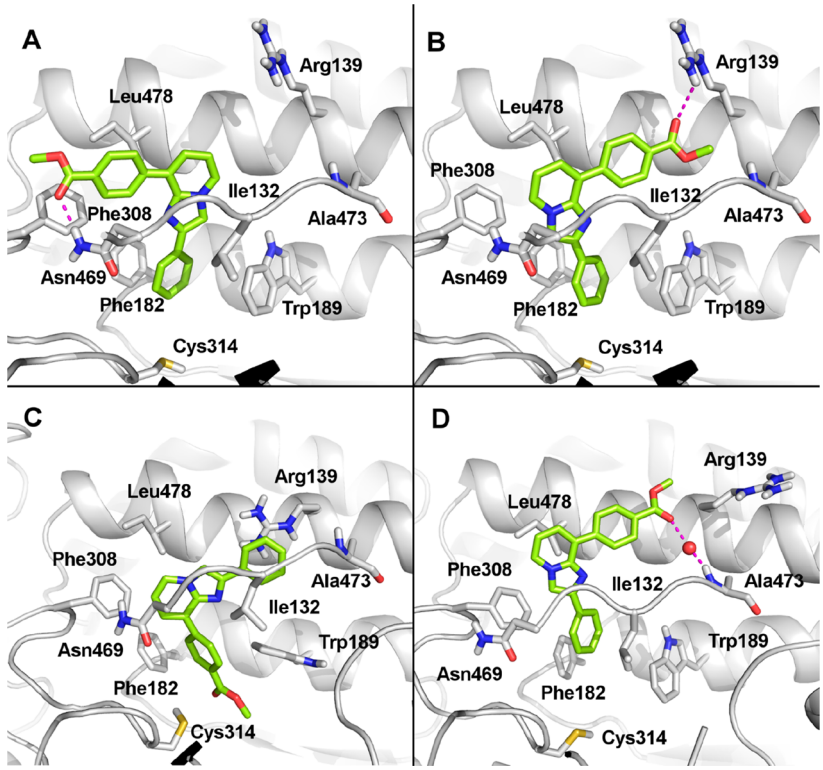

Figure 4. Stick representations of the proposed docking poses (A and B boxes) and representative frames from MD simulations (C and D boxes) of compound **3f** into the binding site of ALDH1A3 (PDB code: 6TRY), represented as gray ribbons. Residues relevant for the inhibitor binding have been labeled, and their side chains are shown as gray sticks.

able to bind ALDH1A3 protruding toward the catalytic C314 residue. Results obtained confirm the soundness of our initial working hypothesis, based on the suitable relocation of the 6-phenyl ring of GA11 to increase the structural complementarity of this class of compounds with the enzyme binding site.

Antiproliferative Study of Derivative 3c. Derivative **3c**, chosen as the representative compound among the most effective inhibitors, was investigated for its antiproliferative efficacy against the U87-MG cell line, used as a model of human glioblastoma overexpressing ALDH1A3[21] and, as reported in Human Atlas, silencing the isoforms ALDH1A1 and ALDH1A2.

https://dx.doi.org/10.1021/acsmedchemlett.9b00686
ACS Med. Chem. Lett. 2020, 11, 963−970

As displayed in Figure 3-SI (Supporting Information), compound **3c** proved to reduce U87-MG vitality, although not significantly, when tested at concentrations in the high micromolar range. To rationalize the observed discrepancy between the cell-free and the cell-based assay results, a prediction of the physiochemical properties of the test compound was carried out using the QikProp program.[22] Despite an estimated good cell permeability (QPPCaco, 8020 nm/s), **3c** was predicted to have a weak water solubility (QPlogS, −6.482) and a relatively high logP (QPlogPo/w, 5.666), although within the range of 95% of current drugs. Accordingly, the low antiproliferative activity observed might be ascribed in principle to the limited water solubility and bioavailability of the compound, which certainly deserves an in depth investigation and optimization.

CONCLUDING REMARKS

It is now clear that the ALDH1A enzyme subfamily, and especially the 1A1 and 1A3 isoforms, play a crucial role in tumor progression and invasion by modulating self-renewing differentiation and expansion of CSCs. Accordingly, compounds able to block their catalytic activity may represent an effective strategy to fight cancer. Pursuing our interest in the field of ALDH inhibitors, and taking advantage of a structure-based optimization, we succeeded in improving the functional activity of a previously developed hit compound (GA11, IC_{50} 4.7 ± 1.7 μM[15]) obtaining the novel lead **3f**, methyl 4-(2-phenylimidazo-[1,2-*a*]pyridin-8-yl)benzoate (IC_{50} 0.66 ± 1.3 μM). Characterized by a distinctive molecular geometry, **3f** proved to bind the catalytic site of ALDH1A3 protruding toward the key C314. Moreover, thanks to the metoxycarbonyl fragment on the 8-phenyl ring, it is able to H-bond the protein backbone, thus settling firmly into the binding site of the target protein. Such a structural complementarity gave reason of its significant functional efficacy. Actually, showing both IC_{50} and K_i values in the sub-micromolar range, **3f** stands out as the most effective ALDH1A3 inhibitor ever described to date. Clearly, thorough investigations in complex structures like cell lines and animal models are now necessary, to prove its robustness as a novel prototype of an anticancer agent.

EXPERIMENTAL PROCEDURES

Chemistry. Melting points were determined using a Reichert Köfler hot-stage apparatus and are uncorrected. Routine ^{1}H NMR and ^{13}C NMR spectra were recorded in DMSO-d_6 solution on a Bruker 400 spectrometer operating at 400 MHz. Evaporation was performed in vacuo (rotary evaporator). Analytical TLCs were carried out on Merck 0.2 mm precoated silica gel aluminum sheets (60 F-254). Purity of the target inhibitors was determined by HPLC analysis, using a Shimadzu LC-20AD liquid chromatograph (PDA, 250−500 nm) and a Luna C18 column (250 mm × 4.6 mm, 5 μm, Phenomenex), with a gradient of 30% water and 70% acetonitrile and a flow rate of 1.0 mL/min. All the compounds showed percent purity values ≥95%. HRMS were obtained with a Q Exactive Plus Hybrid Quadrupole-Orbitrap Mass Spectrometer (Thermo Fisher Scientific). 3-Bromopyridin-2-amine, the suitably substituted 2-bromo-1-phenylethan-1-one, and the appropriate boronic acids, used to obtain the target inhibitors, were from Alfa Aesar, Aldrich, and Fluka. 8-Bromo-2-phenylimidazo[1,2-*a*]pyridine **2a** and 8-bromo-2-(3-methoxyphenyl)imidazo[1,2-*a*]-pyridine **2d** were synthesized following reported procedures.[23]

General Procedure for the Synthesis of 6-Bromo-2-(substituted)phenylimidazo[1,2-*a*]pyridines, 2b,c. A mixture of 5-bromopyridin-2-amine **1** (1.00 mmol), the suitably substituted 2-bromo-1-phenylethan-1-one (1.00 mmol), and potassium carbonate (138 mg, 1.00 mmol) in 20.0 mL of EtOH was refluxed under stirring until the disappearance of the starting material (TLC analysis). After cooling, the crude obtained was evaporated to dryness. Water was then added to the residue and the desired heterocycle, **2b,c**, separated as a white solid, was collected by filtration, purified through recrystallization from the suitable solvent, and characterized with physio-chemical and spectroscopic data (Table 2-SI, Supporting Information).

General Procedure for the Synthesis of 2,8-(Substituted)-diphenylimidazo[1,2-*a*]pyridines, 3a−t. A solution of the appropriate imidazo[1,2-*a*]pyridine derivative **2a−d** (1.00 mmol), $Pd(OAc)_2$ (0.10 mmol) and PPh_3 (0.20 mmol) in toluene was added with the suitable phenyl boronic acid (1.50 mmol), dissolved in ethanol, and 2 mL of Na_2CO_3 2 M. The resulting mixture was refluxed under stirring until the disappearance of the starting material (TLC analysis). After cooling, the crude obtained was evaporated to dryness and the residue was purified by column chromatography (silica gel, ethyl acetate/petroleum ether). The pure product was then recrystallized from the suitable solvent and characterized by physiochemical and spectroscopic data (Table 3-SI, Supporting Information).

ASSOCIATED CONTENT

Supporting Information

The Supporting Information is available free of charge at https://pubs.acs.org/doi/10.1021/acsmedchemlett.9b00686.

Data collection and refinement statistics of the human ALDH1A3 model. Rearrangement of compound **3f** within the catalytic site of ALDH1A3, extrapolated from MD simulation. Conformational stability of the **3f**−ALDH1A3 complex in MD simulations. Overlap of the binding mode of the crystallized compound **3c** and the representative poses of compound **3f** extrapolated from MD trajectories. Antiproliferative activity of compounds **3c** against the U87-MG cell line. Physiochemical and spectroscopic data of compounds **2b,c** and **3a−t**. Experimental procedures of biochemical and antiproliferative assays. Experimental procedures of crystallization and computational studies. PDB ID Code. 6TRY. Authors will release the atomic coordinates and experimental data upon article publication. (PDF)

MD simulation video (MPG)

AUTHOR INFORMATION

Corresponding Authors

Silvia Garavaglia − *Department of Pharmaceutical Sciences, University of Piemonte Orientale, 28100 Novara, Italy*; Email: silvia.garavaglia@uniupo.it

Concettina La Motta − *Department of Pharmacy and CISUP - Centre for Instrumentation Sharing, University of Pisa, 56126 Pisa, Italy*; orcid.org/0000-0002-0194-5431; Email: concettina.lamotta@unipi.it

Authors

Luca Quattrini − *Department of Pharmacy, University of Pisa, 56126 Pisa, Italy*

Edoardo Luigi Maria Gelardi − *Department of Pharmaceutical Sciences, University of Piemonte Orientale, 28100 Novara, Italy*

Giovanni Petrarolo − *Department of Pharmacy, University of Pisa, 56126 Pisa, Italy*

Giorgia Colombo − *Department of Pharmaceutical Sciences, University of Piemonte Orientale, 28100 Novara, Italy*

Davide Maria Ferraris − *Department of Pharmaceutical Sciences, University of Piemonte Orientale, 28100 Novara, Italy*

Francesca Picarazzi − *Department of Biotechnology, Chemistry and Pharmacy "Department of Excellence 2018-2022", University of Siena, 53100 Siena, Italy*

https://dx.doi.org/10.1021/acsmedchemlett.9b00686
ACS Med. Chem. Lett. 2020, 11, 963−970

Menico Rizzi − *Department of Pharmaceutical Sciences, University of Piemonte Orientale, 28100 Novara, Italy*

Complete contact information is available at: https://pubs.acs.org/10.1021/acsmedchemlett.9b00686

Author Contributions

[‖]L.Q. and E.L.M.G. contributed equally to the work.

Notes

The authors declare no competing financial interest.

■ ACKNOWLEDGMENTS

The authors acknowledge Beatrice Muscatello, CISUP (Centre for Instrumentation Sharing - University of Pisa) for HRMS analysis, and the European Synchrotron Radiation Facility (ESRF, Grenoble, France) for data collections at the beamlines ID29. S.G. and D.M.F. acknowledge the University of Piemonte Orientale (grant Ricerca Ateneo FAR_2016) and ROCHE per la Ricerca 2017, for financial support. F.P. acknowledges a MIUR (Ministero dell'Istruzione, dell'Università e della Ricerca) grant "Dipartimento di Eccellenza 2018−2022".

■ ABBREVIATIONS

ALDH, aldehyde dehydrogenase; ALDH1A1, aldehyde dehydrogenase subtype 1A1; ALDH1A2, aldehyde dehydrogenase subtype 1A2; ALDH1A3, aldehyde dehydrogenase subtype 1A3; RA, retinoic acid; ATRA, all-trans retinoic acid; 9-cis-RA, 9-cis retinoic acid; 13-cis-RA, 13-cis retinoic acid; RARE, retinoic acid (RA) response element; GSCs, glioma stem-like cells.

■ REFERENCES

(1) Black, W.; Vasiliou, V. The aldehyde dehydrogenase gene superfamily resource center. *Hum. Genomics* **2009**, *4*, 136−42.

(2) Balmer, J. E.; Blomhoff, R. Gene expression regulation by retinoic acid. *J. Lipid Res.* **2002**, *43*, 1773−808.

(3) Moreb, J. S. Aldehyde dehydrogenase as a marker for stem cells. *Curr. Stem Cell Res. Ther.* **2008**, *3*, 237−246.

(4) Xu, X.; Chai, S.; Wang, P.; Zhang, C.; Yang, Y.; Yang, Y.; Wang, K. Aldehyde dehydrogenases and cancer stem cells. *Cancer Lett.* **2015**, *369*, 50−57.

(5) Ginestier, C.; Hur, M. H.; Charafe-Jauffret, E.; Monville, F.; Dutcher, J.; Brown, M.; Jacquemier, J.; Viens, P.; Kleen, C.; Liu, S.; Schott, A.; Hayes, D.; Birnbaum, D.; Wicha, M. S.; Dontu, G. ALDH1 is a marker of normal and malignant human mammary stem cells and a predictor of poor clinical outcome. *Cell Stem Cell* **2007**, *1*, 555−567.

(6) Pearce, D. J.; Taussig, D.; Simpson, C. Characterization of cells with a high aldehyde dehydrogenase activity from cord blood and acute myeloid leukemia samples. *Stem Cells* **2005**, *23*, 752−760.

(7) Yang, L.; Ren, Y.; Yu, X.; Quian, F.; Bian, B.-S.-J.; Xiao, H.-L.; Wang, W.-G.; Xu, S.-L.; Yang, J.; Cui, W.; Liu, Q.; Wang, Z.; Guo, W.; Xiong, G.; Yang, K.; Quian, C.; Zhang, X.; Zhang, P.; Chi, Y.-H.; Bian, X.-W. ALDH1A1 defines invasive cancer stem-like cells and predicts poor prognosis in patients with esophageal squamous cell carcinoma. *Mod. Pathol.* **2014**, *27*, 775−783.

(8) Li, T.; Su, Y.; Mei, Y.; Leng, Q.; Leng, B.; Liu, Z.; Stass, S. A.; Jiang, F. ALDH1A1 is a marker for malignant prostate stem cells and predictor of prostate cancer patients'outcome. *Lab. Invest.* **2010**, *90*, 234−244.

(9) Meng, E.; Mitra, A.; Tripathi, K.; Finan, M. A.; Scalici, J.; McClellan, S.; Madeira da Silva, L.; Reed, E.; Shevde, L. A.; Palle, K.; Rocconi, R. P. ALDH1A1 maintains ovarian cancer stem cell-like properties by altered regulation of cell cycle checkpoint and DNA repair network signaling. *PLoS One* **2014**, *9*, No. e107142.

(10) Marcato, P.; Dean, C. A.; Liu, R.-Z.; Coyle, K. M.; Bydoun, M.; Wallace, M.; Clemens, D.; Turner, C.; Mathenge, E. G.; Gujar, S. A.; Giacomantonio, C. A.; Mackey, J. R.; Godbout, R.; Lee, P. W. K. Aldehyde dehydrogenase 1A3 influences breast cancer progression via differential retinoic acid signaling. *Mol. Oncol.* **2015**, *9*, 17−31.

(11) Yamashita, D.; Minata, M.; Ibrahim, A. N.; Yamaguchi, S.; Coviello, V.; Bernstock, J. D.; Harada, S.; Cerione, R. A.; Tannous, B. A.; La Motta, C.; Nakano, I. Identification of ALDH1A3 as a viable therapeutic target in breast cancer metastasis-initiating cells. *Mol. Cancer Ther.* **2020**, molcanther.0461.2019.

(12) Shao, C.; Sullivan, J. P.; Girard, L.; Augustyn, A.; Yenerall, P.; Rodriguez-Canales, J.; Liu, H.; Behrens, C.; Shay, J. W.; Wistuba, I. I.; Minna, J. D. Essential role of aldehyde dehydrogenase 1A3 for the maintenance of non-small cell lung cancer stem cells is associated with the STAT3 pathway. *Clin. Cancer Res.* **2014**, *20*, 4154−4166.

(13) Mao, P.; Joshi, K.; Li, J.; Kim, S. H.; Li, P.; Santana-Santos, L.; Luthra, S.; Chandran, U. R.; Benos, P. V.; Smith, L.; Wang, M.; Hu, B.; Cheng, S. Y.; Sobol, R. W.; Nakano, I. Mesenchymal glioma stem cells are maintained by activated glycolytic metabolism involving aldehyde dehydrogenase 1A3. *Proc. Natl. Acad. Sci. U. S. A.* **2013**, *110*, 8644−8649.

(14) Dinavahi, S. S.; Bazewicz, C. G.; Gowda, R.; Robertson, G. P. Aldehyde dehydrogenase inhibitors for cancer therapeutics. *Trends Pharmacol. Sci.* **2019**, *40*, 774−789.

(15) Cheng, P.; Wang, J.; Waghmare, I.; Sartini, S.; Coviello, V.; Zhang, Z.; Kim, S. H.; Mohyeldin, A.; Pavlyukov, M. S.; Minata, M.; Valentim, C. L.; Chhipa, R. R.; Bhat, K. P.; Dasgupta, B.; La Motta, C.; Kango-Singh, M.; Nakano, I. FOXD1-ALDH1A3 signaling is a determinant for the self-renewal and tumorigenicity of mesenchymal glioma stem cells. *Cancer Res.* **2016**, *76*, 7219−7230.

(16) Quattrini, L.; Gelardi, E. L. M.; Coviello, V.; Sartini, S.; Ferraris, D. M.; Mori, M.; Nakano, I.; Garavaglia, S.; La Motta, C. Imidazo[1,2-*a*]pyridine Derivatives as Aldehyde Dehydrogenase Inhibitors: Novel Chemotypes to Target Glioblastoma Stem Cells. *J. Med. Chem.*. Manuscript under revision.

(17) Moretti, A.; Li, J.; Donini, S.; Sobol, R. W.; Rizzi, M.; Garavaglia, S. Crystal structure of human aldehyde dehydrogenase 1A3 complexed with NAD^+ and retinoic acid. *Sci. Rep.* **2016**, *19*, 3571.

(18) Jones, G.; Willett, P.; Glen, R. C.; Leach, A. R.; Taylor, R. Development and validation of a genetic algorithm for flexible docking. *J. Mol. Biol.* **1997**, *267*, 727−748.

(19) Case, D. A.; Ben-Shalom, I. Y.; Brozell, S. R.; Cerutti, D. S.; Cheatham, T. E., III; Cruzeiro, V. W. D.; Darden, T. A.; Duke, R. E.; Ghoreishi, D.; Gilson, M. K.; Gohlke, H.; Goetz, A. W.; Greene, D.; Harris, R.; Homeyer, N.; Izadi, S.; Kovalenko, A.; Kurtzman, T.; Lee, T. S.; LeGrand, S.; Li, P.; Lin, C.; Liu, J.; Luchko, T.; Luo, R.; Mermelstein, D. J.; Merz, K. M.; Miao, Y.; Monard, G.; Nguyen, C.; Nguyen, H.; Omelyan, I.; Onufriev, A.; Pan, F.; Qi, R.; Roe, D. R.; Roitberg, A.; Sagui, C.; Schott-Verdugo, S.; Shen, J.; Simmerling, C. L.; Smith, J.; Salomon-Ferrer, R.; Swails, J.; Walker, R. C.; Wang, J.; Wei, H.; Wolf, R. M.; Wu, X.; Xiao, L.; York, D. M.; Kollman, P. A. *AMBER 2018*; University of California, San Francisco, 2018.

(20) Miller, B. R.; McGee, T. D.; Swails, J. M.; Homeyer, N.; Gohlke, H.; Roitberg, A. E. MMPBSA.py: an efficient program for end-state free energy calculations. *J. Chem. Theory Comput.* **2012**, *8*, 3314−3321.

(21) Zhang, W.; Liu, Y.; Hu, H.; Huang, H.; Bao, Z.; Yang, P.; Wang, Y.; You, G.; Yan, W.; Jiang, T.; Wang, J.; Zhang, W. ALDH1A3: a marker of mesenchymal phenotype in gliomas associated with cell invasion. *PLoS One* **2015**, *10*, No. e0142856.

(22) *Schrödinger Release 2019-4*; QikProp, Schrödinger, LLC: New York, NY, 2019.

(23) Bischoff, F.; Berthelot, D.; De Cleyn, M.; MacDonald, G.; Minne, G.; Oehlrich, D.; Pieters, S.; Surkyn, M.; Trabanco, A. A.; Tresadern, G.; Van Brandt, S.; Velter, I.; Zaja, M.; Borghys, H.; Masungi, C.; Mercken, M.; Gijsen, H. J. M. Design and synthesis of a novel series of bicyclic heterocycles as potent γ-secretase modulators. *J. Med. Chem.* **2012**, *55*, 9089−9106.

(24) Morgan, C. A.; Hurley, T. D. Development of a high-throughput in vitro assay to identify selective inhibitors for human ALDH1A1. *Chem.-Biol. Interact.* **2015**, *234*, 29−37.

(25) Chen, Y.; Zhu, J.-Y.; Hong, K. H.; Mikles, D. C.; Georg, G. I.; Goldstein, A. S.; Amory, J. K.; Schönbrunn, E. Structural basis of

ALDH1A2 inhibition by irreversible and reversible small molecule inhibitors. *ACS Chem. Biol.* **2018**, *13* (3), 582−590.

https://dx.doi.org/10.1021/acsmedchemlett.9b00686
ACS Med. Chem. Lett. 2020, 11, 963−970